# Optical properties of single-crystal sapphire fibers

Rick K. Nubling and James A. Harrington

Single-crystal sapphire fibers have been grown with the laser-heated pedestal-growth method with losses as low as 0.3 dB/m at 2.94 μm. With the incorporation of a computer-controlled feedback system, fibers have been grown with less than ±0.5% diameter variation, or ±1.5 μm for a 300-μm fiber. The losses in these fibers have been reduced further through a postgrowth anneal at 1000 °C in air, from 5.4 to 1.5 dB/m at 543 nm and from 0.4–0.3 dB/m at 2.94 μm. These fibers delivered 4.7 W at 10 Hz of Er:YAG laser power. 

*Key words:* Infrared fibers, sapphire fibers, Er:YAG lasers, optical properties.

## 1. Introduction and Background

Single-crystal (SC) sapphire fibers have many physical properties that make them ideal candidates for infrared transmission as high as ~3.5 μm. Sapphire has an intrinsic (theoretical) loss of 0.13 dB/m at the Er:YAG laser wavelength of 2.94 μm; it has a melting point in excess of 2000 °C; it is chemically inert; and it has the potential of delivering very high laser energies (>1 J/pulse). Furthermore, sapphire fibers are extremely durable and have a distinct advantage in medical applications because they can be safely inserted directly into the body. Because the modulus of sapphire is seven times that of silica, sapphire fibers are fairly stiff; the minimum bend radius of a 300-μm-diameter sapphire fiber is ~45 mm. Sapphire fibers with diameters as high as ~300 μm, however, are quite flexible for most surgical applications.

There are currently two techniques for the growth of SC sapphire fibers. One is the edge-defined, film-fed-growth (EFG) method[1] used by Saphikon, Inc., Milford, N.H.; the other is the laser-heated pedestal-growth (LHPG) method used by researchers at Stanford University,[2,3] the University of South Florida,[4,5] and Rutgers University.[6,7] Chang *et al.* report losses routinely as low as 0.7 dB/m at 2.94 μm in 100-μm-diameter sapphire fibers grown in a helium atmosphere at a rate of 20 mm/min using the LHPG method.[5,8] Saphikon, Inc. has made significant improvements to their EFG sapphire fibers, recently reporting losses as low as 0.2 dB/m at 2.94 μm and averaging 1.5–2.0 dB/m.[9–11] The EFG process allows for multiple fibers to be grown at one time, making it more suitable to production scale-up, but losses still tend to be higher than those routinely grown by the LHPG method. Saphikon, Inc. is currently the only commercial source of optical-quality sapphire fibers.

The LHPG method was first reported by Gasson and Cockayne[12] and Haggerty *et al.*[13–15] for the growth of SC fibers. This process closely resembles the float-zone method of crystal growth in which the crystal rod itself supports the molten zone. LHPG is the most promising method available for the development of high-optical-quality sapphire fibers. The molten zone is held in place by surface tension, eliminating the need for a crucible that could be a possible source of contamination. Furthermore, a $CO_2$ laser beam, which provides a uniform, ultra-clean heat source, is used to melt the starting rod. This growth method allows only one fiber to be grown at a time, so commercialization is difficult. LHPG, however, is the only growth method to routinely produce sapphire fibers with losses approaching theoretical values.

Other infrared transmitting fibers that are good candidates for sensor and power delivery applications include the heavy-metal fluoride and chalcogenide glasses, polycrystalline silver halides, and hollow waveguides.[16] Fluoride glass fibers transmit to ~4.5 μm with losses below 0.05 dB/m at 2.94 μm. In addition to their excellent transparency, they are also quite flexible and have been used to deliver Er:YAG laser fluences as high as 200 J/cm$^2$. However,

When this research was undertaken, the authors were with the Fiber Optic Materials Research Program, Rutgers University, Piscataway, New Jersey 08855. R. K. Nubling is now with Laser Power Optics, Incorporated, San Diego, California 92130.

Received 2 December 1996; revised manuscript received 8 April 1997.

0003-6935/97/245934-07$10.00/0

fluoride glass fibers have major drawbacks: limited mechanical strength, low glass transition temperature (150 °C), and chemical reactivity with water. Chalcogenide glass fibers, made from the chalcogen elements such as As, Ge, Te, S, and Se, transmit beyond 10 μm but they also have low glass transition temperatures. Like the fluoride glasses, they are weak in shear strength which makes them more fragile than sapphire. Silver halide fibers have a large transparency window as high as 20 μm but again they are weak, sensitive to light, and have low melting points. Dielectric-coated, metallic hollow waveguides are excellent candidates for Er:YAG laser power delivery. They have a somewhat larger diameter than most solid-core fibers which can limit their flexibility. Furthermore, hollow waveguides have an additional loss on bending that scales as $\sim 1/R$, where $R$ is the bend radius. Nevertheless, small-bore hollow-glass waveguides, developed by Harrington and his group at Rutgers University, have losses ranging from 0.1–1.73 dB/m and have been used to deliver as much as 8 W at 10 Hz of Er:YAG laser power.[17]

## 2. Laser-Heated, Pedestal Growth of Sapphire Fiber

Most sapphire fibers grown to date by other researchers have been less than 150 μm in diameter.[2,5,18,19] Because of the extremely high-energy density produced on these fiber ends, their use for Er:YAG laser power delivery is limited. In this research, therefore, we focus on the growth of fibers with larger diameters of ~300 μm. A 300-μm-diameter sapphire fiber, although noticeably stiffer than its silica counterpart, is still sufficiently flexible for most applications.

Unfortunately, high-quality, large-diameter sapphire fibers are extremely difficult to grow. Mechanical perturbations are much more easily transmitted from the translation mechanism to the fiber when the fiber diameter is large. These mechanical perturbations can cause fibers to grow curved or with kinks, both of which cause an increase in scattering loss. To circumvent this problem, considerable time and effort were spent in the mechanical design of the LHPG apparatus. A computer-controlled feedback system was added to minimize the diameter fluctuations in the fibers and to prevent axis wander during growth.

### A. Overview of Laser-Heated, Pedestal-Growth Sapphire Fiber Growth

In LHPG SC sapphire fiber growth, a $CO_2$ laser beam is focused onto the tip of a source rod, creating a small molten bead of sapphire. A seed fiber is dipped into the molten region, shown schematically in Fig. 1, and slowly pulled upward forming the SC fiber. The source rod—which may be SC, polycrystalline, sintered, or a pressed powder—is fed upward simultaneously to replenish the supply of molten sapphire. Mass conservation dictates that the diameter reduction be equal to the square root of the fiber-to-source-rod velocity ratio, that is,

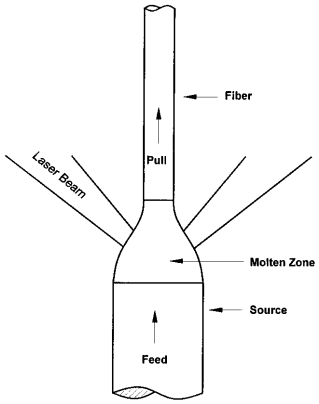


Fig. 1. Schematic diagram of laser-heated pedestal growth illustrating the small molten zone produced in an approximate 3:1 source-rod-to-fiber diameter reduction.

$$\frac{d_s}{d_f} = \sqrt{\frac{v_f}{v_s}},$$

where $d_f$ and $d_s$ are the diameters and $v_f$ and $v_s$ are the velocities of the fiber and source rod, respectively.

The shape of the molten zone is a function of the laser power, the diameter reduction, and the material being grown. The steady-state meniscus angle at the solid–liquid–vapor trijunction is a property of the material being grown[20–23] and for sapphire[18,24] is approximately 17°. We observed similar results during the steady-state growth of our sapphire fibers. Fejer's thermodynamic models of the molten-zone shape during LHPG of sapphire indicate a range of molten-zone lengths that will produce stable growth.[25] Fejer's calculations as well as those of Kim *et al.*[26] suggest a maximum stable zone length of approximately 3× the fiber diameter.

Smooth SC fibers are much more difficult to produce than smooth glass fibers. The viscosity of a glass decreases gradually as it is heated, allowing it to be pulled into a smooth fiber. The viscosity of crystalline material at the molten zone is low and thus sensitive to any minor perturbations in the system. Because the molten region is held in place simply by surface tension, any air currents, vibrations, laser power fluctuations, etc., will have enormous effects on the stability of growth. If the system is perturbed during growth, the fiber diameter will oscillate about its thermodynamic equilibrium value before again reaching a steady state. Although it is possible through careful design to minimize the external disturbances to the system, their elimination is nearly impossible. Fejer predicts that the major factor contributing to diameter fluctuations during growth is an unstable laser source.[25] The period of the oscillations is a function of the molten-zone length. Longer molten zones yield long-range diameter fluctuations whereas shorter molten zones yield short-range diameter fluctuations. The optimal

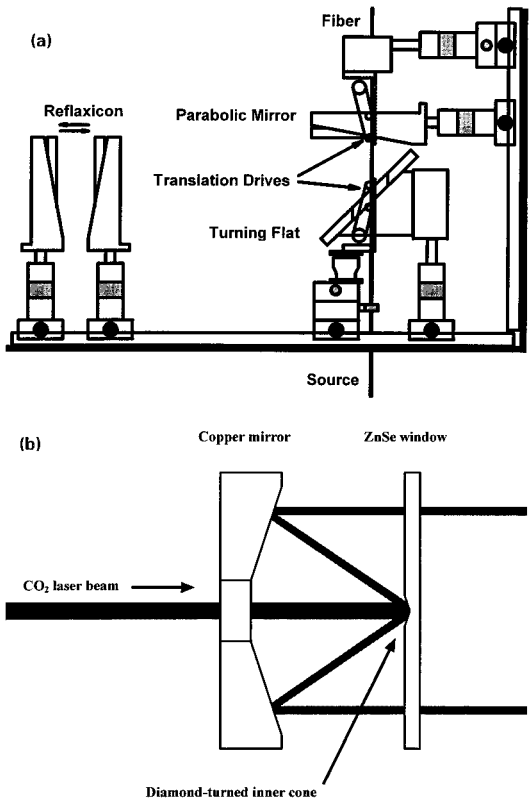


Fig. 2. Schematics of (a) our continuous-feed LHPG apparatus and (b) our reflaxicon optical arrangement. The source rod (as much as 2 m long) is fed through a hole drilled in the table, and the entire system is sealed within an airtight Plexiglas enclosure.

molten-zone length is approximately equal to the diameter of the source rod for a diameter reduction of 3:1.

### B. Details of the Laser-Heated Pedestal-Growth System and Fiber Diameter Control

Our LHPG apparatus, shown in Fig. 2(a), was built to grow fibers 1 m or greater in length. The mechanical drive mechanisms involved the use of dc-motor-driven belt drives to smoothly translate the source rod and seed fibers. A precision V groove in a hard anodized metal block provided the low-friction guiding surface for the sapphire source and fiber. The groove angle was 90°, and the depth depended on the diameter of the fiber or source rod. We found that smaller groove depths—so that slightly more than half the diameter of the fiber or source protruded beyond the surface of the block—provided smoother translation. We also found that using a stainless-steel guide tube, with a bore slightly larger than the fiber diameter and mounted on the end of the fiber translator, helped to eliminate side-to-side motion. The diameter of the fiber was measured in line by a LaserMike, Inc. laser micrometer, with a resolution of $<0.1$ μm, which was fitted with a notch filter so that the detector was not saturated by the intense white light from the molten sapphire. The measurements from the laser micrometer were fed to the computer and used in a feedback loop to precisely control the fiber diameter during growth. The laser source used was a Coherent Model 42 flowing-gas $CO_2$ laser. This laser could deliver as much as 50 W of near $TEM_{00}$ power. The 10-mm-diameter output beam was expanded to ~16 mm and directed into the reflaxicon optical arrangement shown schematically in Fig. 2(b). Normally the power stability of this laser is ±5% with temperature-controlled cooling water. Because this is too large an amplitude fluctuation for fiber growth, we added a feedback system to control electronically the laser power. Using this feedback system, we were able to stabilize the laser power to ±0.5%. Typically, 10 W was needed to melt our 1-mm-diameter source rods, and the power fluctuation was less than ±0.05 W. Finally, the entire system was sealed within a Plexiglas enclosure to block out any air currents that could disrupt the growth process and to allow for growth in different atmospheres. Source rods were obtained from Saphikon, Inc., in lengths as long as 2 m. Use of this length of source rod and a 3:1 diameter reduction would enable us, in principle, to grow fibers as long as 15 m.

The optical system used to focus a ring of laser light onto the source rod employed the following elements: a reflaxicon, a turning flat, and a parabolic mirror. The second element of the reflaxicon was made out of a ZnSe window with a Ag-coated, diamond-turned cone in the center. By using a window and reflecting cone, we eliminated the need for supporting spokes for the cone and thus our laser beam was not obscured. The entire optical system could produce a calculated spot size as small as 22 μm. In practice, however, we adjusted the spacing between the reflaxicon elements so that we could produce a larger focused spot that led to more stable growth from the large 1-mm-diameter source rods.

The control of fiber diameter was crucial to the growth of uniform, low-loss fiber. Our LHPG apparatus was controlled by a Labview program that simultaneously monitored and controlled the fiber diameter and laser power, each to more than ±0.5% stability. All control and process variables were recorded automatically during growth, and the program could also automatically stop fiber growth if necessary. At the typical growth rate of 2 mm/min, a 1-m-long fiber took nearly 8.5 h to grow. The longest fiber was 5 m, which took nearly 40 h to grow. Figure 3 shows the dramatic improvement to diameter stability as a result of the computer-controlled feedback. Without the feedback, diameter fluctuations were ~±5% (i.e., ±15 μm for a 300-μm-diameter fiber); a factor of 10 higher than achieved with the feedback. We were able to grow 300-μm-diameter fibers with peak-to-peak diameter fluctuations less than 2 μm.

## 3. Results and Discussion of the Optical Properties of Laser-Heated Pedestal-Growth Sapphire Fibers

### A. Intrinsic Loss

The intrinsic or theoretical losses for bulk sapphire are a combination of the Urbach edge, Brillouin scat-

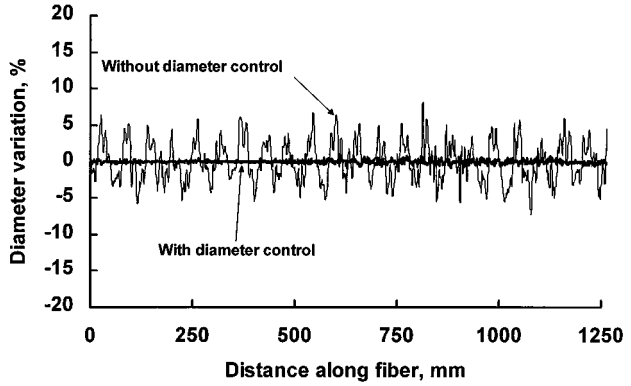


Fig. 3. Diameter fluctuations in LHPG sapphire fibers with and without active feedback control.

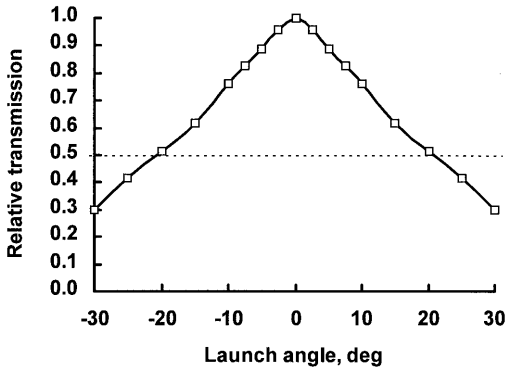


Fig. 5. Effective NA of 300-μm-diameter sapphire fiber.

tering, and multiphonon absorption. In Fig. 4 we plotted data from Thomas and Tropf on the Urbach[27] and from Thomas on the multiphonon[28] absorption edges in sapphire along with the calculated Brillouin scattering losses for sapphire using the relationship given by Rich and Pinnow.[29] When the data are plotted as in Fig. 4 they reveal the characteristic V-curve relationship for loss in transparent materials. From the data in Fig. 4 we can obtain the minimum attenuation coefficient (minimum in the V curve) for sapphire, which is approximately $8 \times 10^{-9}$ $cm^{-1}$ or $3.4 \times 10^{-3}$ dB/km at 1.78 μm. The measured loss for bulk sapphire is, however, many orders of magnitude higher than this minimum intrinsic value. In Fig. 4 we also plotted the experimental data taken from Innocenzi *et al.*[30] for high-purity bulk sapphire. Comparing the measured results with the intrinsic loss, we note that the bulk data differ significantly from the theoretical loss over most of the visible and near-IR region of the spectrum. This is normally the case for crystalline materials in contrast to fused silica for which the measured losses are in close agreement to those calculated for Rayleigh scattering and multiphonon absorption. Interestingly, we can fit Innocenzi *et al.* data to a power-law varying as $\lambda^{-4}$ for wavelengths below ~1.5 μm (solid curve through data points in Fig. 4). This suggests that Rayleigh scattering from inhomogeneities in the crystal contributes to the extrinsic loss. We also estimate from the data in Fig. 4 the intrinsic loss at 2.94 μm. By extrapolation of the multiphonon absorption losses we find a loss of ~0.13 dB/m at 2.94 μm.

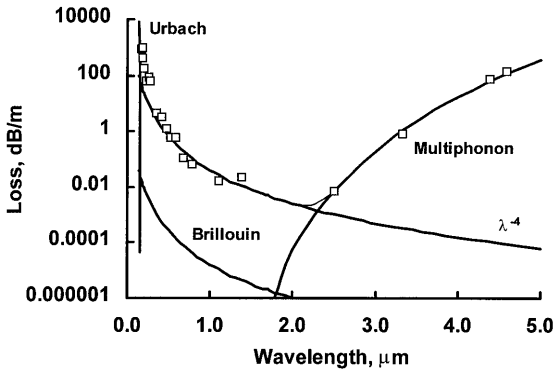


Fig. 4. Bulk attenuation in sapphire. Open boxes, data taken from Innocenzi *et al.*[30]

### B. Effective Numerical Aperture of Fiber

The theoretical numerical aperture (NA) of a step index fiber is given by a NA of $(n_{co}^2 - n_{cl}^2)^{1/2}$, where $n_{co}$ and $n_{cl}$ are the refractive indices of the core and cladding, respectively. As a core-only fiber with an index ~1.72, sapphire will have a theoretical NA >1. This would suggest that sapphire fibers will transmit all rays incident on the input face regardless of the launch angle. In practice, however, we find this is not the case since bulk and surface defects scatter the light into large-angle lossy modes. As a result we use an effective numerical aperture, $NA_{eff}$, to better describe the true launch constraints. The $NA_{eff}$ is defined as the sine of the launch angle at which the transmission drops to 50% of the transmission with a 0° launch angle. We determined the $NA_{eff}$ at 2.94 μm by measuring the transmission as a function of the launch angle with a collimated input beam from an Er:YAG laser. The NA measurement of a typical 300-μm-diameter LHPG sapphire fiber is shown in Fig. 5. From this data, we obtain a $NA_{eff} \cong 0.35$ for our fiber.

### C. Fiber Loss

Loss measurements of our LHPG fibers were made at discrete wavelengths with Ar-ion, He–Ne, and Er:YAG lasers. All the lasers (except for the 1.15-μm He–Ne) had single-mode outputs or were apertured to produce nearly a single mode. Broadband, spectral loss measurements were made with a combination of an Ando spectrum analyzer, a Perkin-Elmer Lambda 9 spectrometer, and a Perkin-Elmer Model 1725X FTIR spectrometer with a $LN_2$-cooled InSb detector. All spectral and laser measurements were made by the cut-back method to remove coupling losses.

Scattering measurements were done in the visible with He–Ne lasers. A 1-in.(2.54-cm)-diameter integrating sphere was used for the scattering measurements, and data were taken along the length of the fibers to identify any hot spots or regions of abnormally high scattering. The differential light scat-

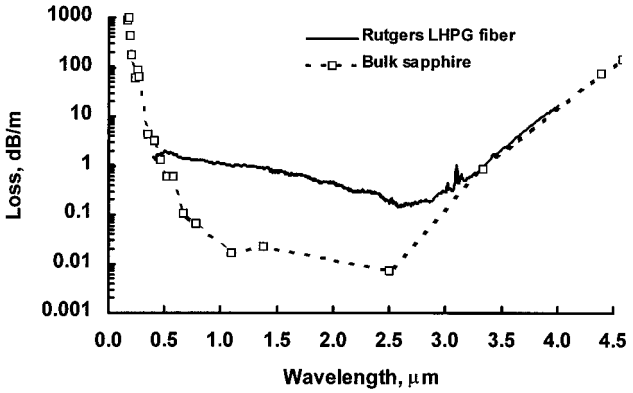


Fig. 6. Visible IR spectrum of 300-μm-diameter sapphire fiber compared with the bulk data of Innocenzi *et al.*[30]

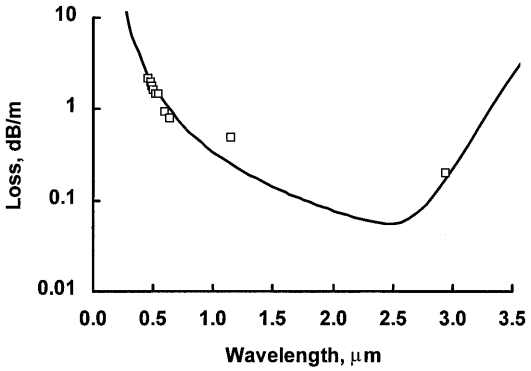


Fig. 7. Laser measurements of attenuation of a 300-μm-diameter sapphire fiber. The solid curve is a fit to the data when a $\lambda^{-2}$ contribution is added to the bulk loss.

tered into the integrating sphere $dI_s$ from a length $dx$ of fiber at a distance $x$ from the input end of the fiber is given by[31]

$$dI_s = I(x)\alpha_s dx. \tag{1}$$

Assuming a constant total attenuation $\alpha_T$ along the length, we can express the intensity at a distance $x$ from the input end $I(x)$ as

$$I(x) = (1 - R)I_0 \exp(-\alpha_T x), \tag{2}$$

where $R$ is the single-surface reflectance of sapphire, so that Eq. (1) can be written[32]

$$dI_s = \alpha_s(1 - R)I_0 \exp(-\alpha_T x)dx. \tag{3}$$

Integration from $x - D/2$ to $x + D/2$, where the sphere of diameter $D$ is centered at $x$, yields

$$I_s = \frac{\alpha_s}{\alpha_T}(1 - R)I_0\left[\exp\left(\alpha_T \frac{D}{2}\right) - \exp\left(-\alpha_T \frac{D}{2}\right)\right]\exp(-\alpha_T x). \tag{4}$$

The output power $I_{\text{out}}$ can be expressed as

$$I_{\text{out}} = (1 - R)^2 I_0 \exp(-\alpha_T x)\exp[-\alpha_T(L - x)], \tag{5}$$

where $L$ is the fiber length. The combination of Eq. (4) and (5) yields

$$\alpha_s = \alpha_T(1 - R)\left\{\exp\left[\alpha_T\left(L - x + \frac{D}{2}\right)\right] - \exp\left[\alpha_T\left(L - x - \frac{D}{2}\right)\right]\right\}^{-1} \frac{I_s}{I_{\text{out}}} \tag{6}$$

for the differential scattering coefficient at a distance $x$ from the input end of the fiber. Use of this form of the equation allowed us to calculate the scattering loss along the length of the fiber. We measured the total attenuation $\alpha_T$ using the cut-back method.

The spectral attenuation of one of our best 300-μm-diameter, 1-m-long sapphire fibers is shown in Fig. 6. This fiber was grown under computer control at 2 mm/min in air and had diameter fluctuations less than ±0.5%. In addition, the fiber was annealed in air at 1000 °C for 12 h after growth. The losses are higher than the bulk data of Innocenzi *et al.* below 3 μm. However, at 2.94 μm the loss in this fiber is ~0.3 dB/m, which is approaching the theoretical limit of ~0.13 dB/m. This is one of the lowest losses obtained at 2.94 μm in a SC sapphire fiber. We attribute this low loss to the elimination of crystal imperfections caused by instabilities in the growth process and good diameter control.

Figure 7 shows the laser measurements for the fiber shown in Fig. 6. The solid curve is a fit to this data. The curve fit includes the long wavelength, multiphonon term and a short wavelength $\lambda^{-2}$ contribution. The $\lambda^{-2}$ dependence suggests that the scattering is dominated by Rayleigh–Gans or Mie mechanisms rather than by Rayleigh scattering.[32,33] Rayleigh–Gans scattering has been shown to occur in some polycrystalline IR fibers when the bulk defects are large in the transverse dimension compared to the wavelength of light but small in optical path difference. A further strong indication that the main scattering mechanism is Rayleigh–Gans is the large degree of forward scattering that we observed.[33] Rayleigh scattering is directed into all angles, whereas Rayleigh–Gans is directed into small forward angles. Data taken with a scattering sphere at 633 nm are shown in Fig. 8 for two fibers with large and small total losses. From the data in Fig. 8 we can see that there is an increase in the scattering coefficient as the scattering sphere is moved to the output end of the fiber. This is particularly evident for the high-loss fiber as well as for the low-loss fiber if the hot spot in the center of the fiber is ignored. Normally, if Rayleigh scattering dominates, the scattering coefficient should be nearly constant with the position along the fiber. In our case, however, the increase in $\alpha_s$ with increasing $x$ indicates that forward scattering is the major contribution to the loss. Finally, we note that the best fiber's scattering loss is quite low as a result of the careful control of fiber growth. Presumably we have eliminated many of the scattering sites, such as bubbles and diameter fluctuations present in the high-loss fiber.

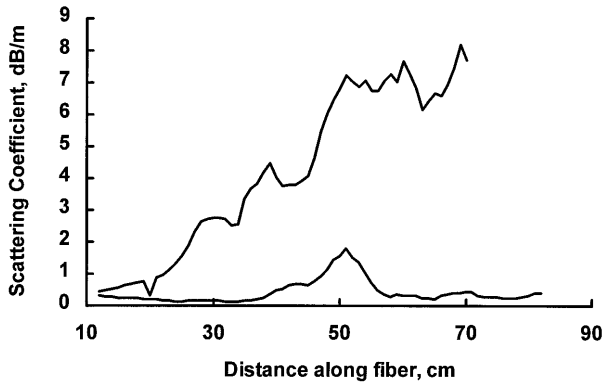


Fig. 8. Scattering loss at 633 nm as a function of distance along two sapphire fibers with different total losses.

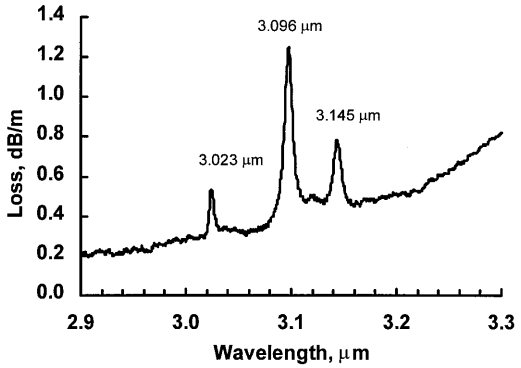


Fig. 10. Three micrometer absorption peaks in our lowest-loss sapphire fiber.

Annealing of sapphire fibers in either air or $O_2$ has been shown to improve dramatically the transmission in the visible region.[34,35] We have seen similar results at short wavelengths after an anneal in air at 1000 °C. Somewhat surprisingly, however, we also see a decrease in loss at 2.94 μm after the annealing process. The spectral and laser loss results for a before- and after-annealed fiber are shown in Fig. 9. The loss in the visible is dominated by an absorption peak at ~410 nm which is due to a V center. This V-center absorption peak has been seen in bulk sapphire[36,37] as well as sapphire fibers[2,34] and is associated with a trapped hole pair on an $O^{2-}$ adjacent to an $Al^{3+}$ vacancy. This V-center defect can be annealed out at a few hundred degrees Celsius.[36] There is also the possibility of a $V_{OH}$ center, which is a V center partially charge compensated by $OH^-$ impurities in the crystal. The fundamental stretching band for an $OH^-$ impurity occurs near 3 μm.[36] Our fibers show both the absorption peak at 410 nm and peaks at 3 μm. We suspect that we may be creating hole centers and introducing $OH^-$ impurities during growth.

The sharp peaks near 3 μm indicate transition metal impurities in our fibers. These impurity bands are reduced drastically through annealing. In Fig. 10 we show the three impurity peaks on an expanded scale. Eigenmann *et al.* observed the same identical peaks in Fe-doped sapphire[38,39] and also demonstrated a reduction in peak intensity when the sample was annealed in $O_2$. Eigenmann *et al.* also noted that the peaks would reappear if the anneal was carried out in a $H_2$ atmosphere and that they would shift to longer wavelengths if annealed in deuterium,[38] proving the hypothesis that the peaks are a result of the O—H and/or O—H—O vibration modes.

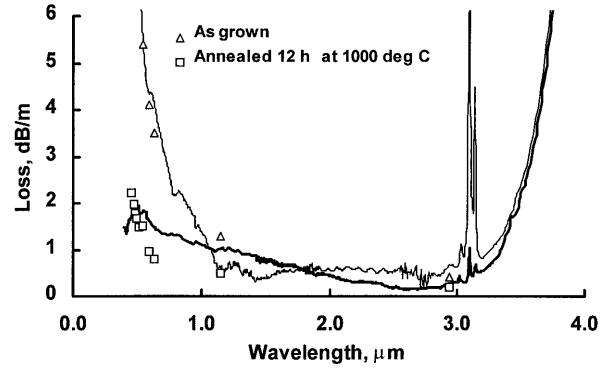


Fig. 9. Spectral loss of 300-μm-diameter sapphire fiber before and after a 12-h anneal in air.

## 4. Conclusions

The optical quality of our SC sapphire fibers has improved considerably during the course of this research. Fibers with losses less than 0.5 dB/m at 2.94 μm and ~3.0 dB/m at 0.633 μm are now grown routinely. Through a postgrowth anneal, we were able to reduce the losses in the visible region to an average of ~1.0 dB/m at 0.633 μm.

The losses in our fibers approach theoretical limits in the wavelength range beyond 3 μm, where multiphonon absorption is the major contributor to loss, but below that range, losses are still considerably higher than theory predicts. Much of the loss between 1 and 3 μm can be attributed to a Rayleigh–Gans-type internal scattering, as is evident by the $\lambda^{-2}$ dependence of attenuation and the strong forward scattering observed. By refinements of the mechanical system we hope to reduce further this internal scattering. Nevertheless, the computer-control system was critical to the growth of high-quality fibers. The peak-to-peak diameter fluctuations were reduced to below ±0.5% and crystallographic axis wander was all but eliminated.

Sapphire fibers are potentially an ideal fiber for laser power delivery because they have a high melting point compared to other nonsilica fibers. In tests of our low-loss (~0.3-dB/m) fiber using a multimode Er:YAG laser, we were able to launch 10 W at 10 Hz (1 J) of laser energy into our fiber with only minimal input-end damage.

## References

1. H. E. LaBelle, Jr., "EFG, the invention and application to sapphire growth," J. Cryst. Growth **50,** 8–17 (1980).
2. D. H. Jundt, M. M. Fejer, and R. L. Byer, "Characterization of

single-crystal sapphire fibers for optical power delivery systems," Appl. Phys. Lett. **55,** 2170–2172 (1989).
3. R. S. Feigelson, "Pulling optical fibers," J. Cryst. Growth **79,** 669–680 (1986).
4. R. S. F. Chang, S. Sengupta, G. J. Dixon, L. B. Shaw, and N. Djeu, "Growth of small laser crystals for study of energy kinetics and spectroscopy," in *Growth, Characterization, and Applications of Laser Host and Nonlinear Crystals*, T. J. Lin, ed., SPIE **1104,** 244–250 (1989).
5. R. S. F. Chang, V. Phomsakha, and N. Djeu, "Recent advances in sapphire fibers," in *Biomedical Optoelectronic Instrumentation*, A. Katzir, J. A. Harrington, and D. M. Harris, eds., SPIE **2396,** 48–53 (1995).
6. G. N. Merberg and J. A. Harrington, "Optical and mechanical properties of single-crystal sapphire optical fibers," Appl. Opt. **32,** 3201–3209 (1993).
7. R. K. Nubling, R. L. Kozodoy, and J. A. Harrington, "Optical properties of clad and unclad sapphire fiber," in *Biomedical Fiber Optic Instrumentation*, J. A. Harrington, D. M. Harris, A. Katzir, and F. P. Milanovich, eds., SPIE **2131,** 56–61 (1994).
8. V. Phomsakha, R. S. F. Chang, and N. Djeu, "Novel implementation of laser heated pedestal growth for the rapid drawing of sapphire fibers," Rev. Sci. Instrum. **65,** 3860–3861 (1994).
9. G. M. Clarke, D. Chadwick, R. K. Nubling, and J. A. Harrington, "Sapphire fibers for three micron delivery systems," in *Biomedical Optoelectronic Instrumentation*, A. Katzir, J. A. Harrington, and D. M. Harris, eds., SPIE **2396,** 54–59 (1995).
10. J. J. Fitzgibbon, H. E. Bates, A. P. Pryshlak, and J. R. Dugan, "Sapphire optical fibers for the delivery of Erbium:YAG laser energy," in *Biomedical Optoelectronic Instrumentation*, A. Katzir, J. A. Harrington, and D. M. Harris, eds., SPIE **2396,** 60–70 (1995).
11. A. P. Pryshlak, J. R. Dugan, and J. J. Fitzgibbon, "Advancements in sapphire optical fibers for the delivery of Er:YAG laser energy and IR sensor applications," in *Biomedical Fiber Optics*, A. Katzir and J. A. Harrington, eds., SPIE **2677,** 35–42 (1996).
12. D. B. Gasson and B. Cockayne, "Oxide crystal growth using gas lasers," J. Mater. Sci. **5,** 100–104 (1970).
13. J. S. Haggerty, "Production of fibers by a floating zone fiber drawing technique," NASA Contract Rep. NASA-CR-120948. (NASA, Greenbelt, Md., 1972).
14. J. S. Haggerty, W. P. Menashi, and J. F. Wenekus, "Method for forming refractory fibers by laser energy," U.S. patent 3,944,640 (16 March 1976).
15. J. S. Haggerty, W. P. Menashi, and J. F. Wenekus, "Apparatus for forming refractory fibers," U.S. patent 4,012,213 (15 March 1977).
16. J. A. Harrington, *Selected Papers on Infrared Fiber Optics*, Milestone Series, Vol. MS-9 (SPIE Press, Bellingham, Wash., 1990).
17. R. L. Kozodoy, A. T. Pagkalinawan, and J. A. Harrington, "Small-bore hollow waveguides for delivery of 3-μm laser radiation," Appl. Opt. **35,** 1077–1082 (1996).
18. M. M. Fejer, J. L. Nightingale, G. A. Magel, and R. L. Byer, "Laser-heated miniature pedestal growth apparatus for single-crystal optical fibers," Rev. Sci. Instrum. **55,** 1791–1796 (1984).
19. R. W. Waynant, S. Oshry, and M. Fink, "Infrared measurements of sapphire fibers for medical applications," Appl. Opt. **32,** 390–392 (1993).
20. T. Surek, "Theory of shape stability in crystal growth from the melt," J. Appl. Phys. **47,** 4384–4393 (1976).
21. T. Surek and B. Chalmers, "The direction of growth of the surface of a crystal in contact with its melt," J. Cryst. Growth **29,** 1–11 (1975).
22. S. R. Coriell and M. R. Cordes, "Theory of molten zone shape and stability," J. Cryst. Growth **42,** 466–472 (1977).
23. T. Surek, S. R. Coriell, and B. Chalmers, "The growth of shaped crystals from the melt," J. Cryst. Growth **50,** 21–32 (1980).
24. A. B. Dreeben, K. M. Kim, and A. Schujko, "Measurement of meniscus angle in laser-heated float zone growth of constant diameter sapphire crystals." J. Cryst. Growth **50,** 126–132 (1980).
25. M. M. Fejer, "Single crystal fibers: growth dynamics and nonlinear optical interactions," Ph.D. dissertation (Stanford University, Stanford, Calif., 1986).
26. K. M. Kim, A. B. Dreeben, and A. Schujko, "Maximum stable zone length in float-zone growth of small diameter sapphire and silicon crystals," J. Appl. Phys. **50,** 4472–4474 (1979).
27. M. E. Thomas and W. J. Tropf, "Vacuum-ultraviolet characterization of sapphire, ALON, and spinel near the band gap," Opt. Eng. **32,** 1340–1343 (1993).
28. M. E. Thomas, "Infrared properties of the extraordinary ray multiphonon processes in sapphire," Appl. Opt. **28,** 3277–3278 (1989).
29. T. C. Rich and D. A. Pinnow, "Total optical attenuation in bulk fused silica," Appl. Phys. Lett. **20,** 264–266 (1972).
30. M. E. Innocenzi, R. T. Swimm, M. Bass, R. H. French, A. B. Vilaverde, and M. R. Kokta, "Room-temperature optical absorption in undoped $\alpha$-$Al_2O_3$," J. Appl. Phys. **67,** 7542–7546 (1990).
31. A. R. Tynes, A. D. Pearson, and D. L. Bisbee, J. Opt. Soc. Am. "Loss mechanisms and measurements in clad glass fibers and bulk glass," **61,** 143–153 (1971).
32. J. A. Harrington and A. G. Standlee, "Attenuation at 10.6 μm in loaded and unloaded polycrystalline KRS-5 fibers," Appl. Opt. **22,** 3073–3078 (1983).
33. A. Sa'ar and A. Katzir, "Scattering effects in crystalline infrared fibers," J. Opt. Soc. Am. A **5,** 832–833 (1988).
34. R. S. F. Chang, Z. Ge, and N. Djeu, "UV-visible transmission characteristics of sapphire fibers grown by laser-heated pedestal growth technique," in *Biomedical Optoelectronic Instrumentation*, A. Katzir, J. A. Harrington, and D. M. Harris, eds., SPIE **2396,** 145–150 (1995).
35. R. S. F. Chang, "Development of high optical quality high temperature sapphire fibers," NASA Final Report NAS1-19508 (NASA, Langley Research Center, Hampton, Va., 1994).
36. T. J. Turner and J. H. Crawford, Jr., "V centers in single crystal $Al_2O_3$," Solid State Commun. **17,** 167–169 (1975).
37. K. H. Lee, G. E. Holmberg, and J. H. Crawford, Jr., "Hole centers in gamma-irradiated, oxidized $Al_2O_3$," Solid State Commun. **20,** 183–185 (1976).
38. K. Eigenmann, K. Kurtz, and H. H. Gunthard, "Solid state reactions and defects in doped verneuil sapphire," Helv. Phys. Acta **45,** 452–480 (1972).
39. K. Eigenmann and H. H. Gunthard, "Valence state, redox reactions and biparticle formation of Fe and Ti doped sapphire," Chem. Phys. Lett. **13,** 58–61 (1972).